HHS Public Access

Author manuscript

Radiat Res. Author manuscript; available in PMC 2021 June 01.

Published in final edited form as:

Radiat Res. 2020 December 01; 194(6): 688–697. doi:10.1667/RADE-20-00065.1.

Evidence for Early Stage Anti-Tumor Immunity Elicited by Spatially Fractionated Radiotherapy-Immunotherapy Combinations

Andrew J. Johnsrud[a,1], **Samir V. Jenkins**[b], **A Jamshidi-Parsian**[b], **Charles M. Quick**[c], **Edvaldo P. Galhardo**[b], **Ruud P.M. Dings**[b], **Kieng B. Vang**[d], **Ganesh Narayanasamy**[b], **Issam Makhoul**[a], **Robert J. Griffin**[b,1]

[a]Division of Hematology and Oncology, University of Arkansas, Little Rock, Arkansas

[b]Departments of Radiation Oncology University of Arkansas, Little Rock, Arkansas

[c]Departments of Pathology University of Arkansas, Little Rock, Arkansas

[d]Center for Integrative Nanotechnology Sciences, University of Arkansas, Little Rock, Arkansas

Abstract

The combination of radiotherapy and immunotherapy may generate synergistic anti-tumor host immune responses and promote abscopal effects. Spatial fractionation of a radiation dose has been found to promote unique physiological responses of tumors, which might promote synergy with immunotherapy. To determine whether spatial fractionation may augment immune activity, whole-tumor or spatial fractionation grid radiation treatment (GRID) alone or in combination with antibodies against immune checkpoints PD1 and CTLA-4 were tested in an immunocompetent mouse model using a triple negative breast tumor (4T1). Tumor growth delay, immuno-histochemistry and flow cytometry were used to characterize the effects of each treatment type. Whole-beam radiation with immune checkpoint inhibition significantly restrained tumor growth in the irradiated tumor, but not abscopal tumors, compared to either of these treatments alone. In mice that received spatially fractionated irradiation, evidence of abscopal immune responses were observed in contralateral tumors with markedly enhanced infiltration of both antigen-presenting cells and activated T cells, which were preceded by increased systemic IFNγ production and led to eventual tumor growth delay. These studies suggest that systemic immune activation may be triggered by employing GRID to a primary tumor lesion, promoting anti-tumor immune responses outside the treatment field. Interestingly, PD-L1 was found to be upregulated in abscopal tumors from GRID-treated mice. Combined radio-immunotherapy therapy is becoming a validated and novel approach in the treatment of cancer. With the potential increased benefit of GRID to augment both local and metastatic disease responses, further exploration of GRID treatment as a part of current standards of care is warranted.

[1]Address for correspondence: 1087 Tanland Dr., Unit 101, Palo, Alto, CA 94303; Andyj330@stanford.edu or RJGriffin@uams.edu.

INTRODUCTION

As treatment paradigms evolve, an expanding role for radiotherapy in the systemic management of cancer is becoming more evident in the pre-clinical literature and in sporadic human case studies (1-3). While advances in sophistication and highly conformal techniques have enabled precise local treatment, it is also now acknowledged that radiation recruits biologic effectors from outside of the treatment field that lead to bystander effects, including immunologic responses both in the irradiated volume and in distant, nonirradiated lesions (4). With the inclusion of immunotherapy alone into our therapeutic armamentarium at varying levels of success, utilization of radiotherapy to enhance anti-tumor responses represents a new frontier with tremendous potential. Various combination strategies using radiotherapy and immunotherapy are undergoing investigation, showing success in pre-clinical models (5-8) and large clinical trials (9). These findings raise interest in the potential generation of abscopal effects (outside the radiation field) which are likely to be immune-mediated (10). Such events have been observed with radiation exposure, albeit infrequently, since as early as 1953 (11). There are also reported studies, including from our group, describing abscopal phenomena in normal tissues after partial organ or body irradiation (12-14). The mechanisms are not completely understood but are presumed to involve complex immune interactions promoted by generation of tumor-associated antigens and release of cytokines due to radiation damage to stromal and parenchymal cells (7). Such processes have been shown to enhance T-cell repertoire diversity and tumor-specific systemic immune responses (6, 10, 15). Additional components of the process are likely to involve molecular alterations to the tumor microenvironment, intratumoral blood flow, and systemic T-cell trafficking (16, 17). In recently published clinical studies, abscopal events have been observed (18-20), often in highly immunogenic tumors or with concomitant immune checkpoint inhibitor treatment. A clinical role for such combinations has not been defined, and it remains unclear how to synergize these effects.

It is conceivable that alternative methods of radiation delivery might induce unique systemic effects due to the varying damage induced by dose or spatial placement of the beams, and it has been suggested that different dose and fractionation schedules may be a route to more consistent generation of abscopal responses (21, 22). It has also been shown that external beam radiation to a target lesion may be sufficient to deplete a majority of circulating naïve T cells at critical points of cross-presentation, abrogating the development of effective immunologic anti-tumor activity and potentially precluding the evolution of abscopal effects (23). These findings suggest that spatial fractionation grid radiation treatment (GRID) as a component of combination radio-immunotherapy may create interspersed areas of intratumoral immune cell sparing and vascular access with the potential for better immune system activation. This technique was described initially in 1909 by Kohler (24) and developed later to deliver a high-dose fraction to a large treatment area divided into small fields with steep dose gradients, with the initial intention to optimize destruction of bulky tumors with minimal normal tissue effects (25-28). Interestingly, spatial fractionation may also modulate systemic responses owing to the unique interactions between irradiated and nonirradiated tissue volumes which can regulate cytokine production/access to the

circulation and induce bystander effects (29). Similar effects have been observed with the use of partial volume irradiation in some models (30).

Based on these observations we postulated that spatial fractionation with a single GRID dose of 20 Gy may provide a unique stimulus to instigate systemic immune responses that act on distant, nonirradiated tumors and provide a novel platform for combined radio-immunotherapy. The objectives of this study were to observe and compare the early changes in composition of immune cell tumor infiltrates over a few weeks postirradiation. We assessed changes in systemic signals of immune activation in mice treated with a single 20 Gy field that covers the whole primary tumor (whole-beam, WTRT) or with the GRID collimator using a honeycomb beam pattern of 2-mm openings that delivered 20 Gy and 4 mm center to center distance. We also combined the irradiations with dual immune checkpoint blockade by antibody treatment, and analyzed the tumor growth in both primary and abscopal (nonirradiated) tumors and immune cell infiltration in the abscopal tumor. Included in our analysis is a subset of mice where inoculation of a nonirradiated site was delayed until the day of primary tumor irradiation. This was done with the intention to allow study of a longer growth delay period for the primary tumor and a developing metastatic or secondary lesion before either tumor grew past the limits of acceptable size, according to our approved animal use protocol.

MATERIALS AND METHODS

Cell Culture

4T1 murine breast carcinoma cells (ATCC® CRL-2539; Gaithersburg, MD) were cultured in DMEM supplemented with 10% fetal bovine serum (FBS; Atlanta Biologicals, Norcross, GA) and 1% penn/strep (Gibco®, Grand Island, NY). Cells were kept in a humidified incubator at 37°C and 5% CO_2 and passaged twice a week.

Tumor Inoculation

Female Balb/C mice were purchased from Jackson Laboratory (Bar Harbor, ME) and randomly divided into two groups at approximately 12 weeks of age. 4T1 cells were injected subcutaneously into both the right and left rear limbs of the animal. In the first group both limbs were inoculated five days before irradiation. In the second group the right limb was inoculated five days prior to irradiation while the left limb was inoculated on the same day as irradiation. Approximately 100,000 cells were injected into the right and 50,000 into the left limb. The tumor size was measured every two or three days using a metric scale caliper and the volume was estimated by using the formula $(a^2 b)/2$, where a and b are the width and length dimensions of the tumor, respectively.

Irradiation Procedure

Tumors were observed until reaching an approximate volume of 150–200 mm^3. The right-side tumor was deemed as the primary tumor and was irradiated with a single dose of 20 Gy as either whole-tumor radiation or spatially fractionated radiation using a collimator, as shown in Fig. 1B. The GRID collimator was approximately 1.1 cm in diameter and completely covered the tumor volume. Irradiations were performed using an in-house small

animal irradiator (31) at 225 kV, 13 mA, dose rate of approximately 1.31 Gy/min with the whole beam, and 1.03 Gy/min with the GRID collimator. The irradiation field was defined using Gafchromic™ film prior to introduction of animals, and mice were sequentially placed with laser-guided positioning so that only the primary tumor was in the field. Irradiation using a honeycomb grid pattern on Gafchromic EBT2 film (Radiation Products Design Inc., Albertville, MN) placed at the isocenter followed by measurements using ImageJ version 1.49v (National Institutes of Health, Bethesda, MD) yielded a valley-to-peak ratio of 0.3. This is consistent with published data on grid radiotherapy plans (32). The abscopal tumor was not irradiated.

After irradiation mice were either observed or treated accordingly with immune checkpoint inhibitor (ICI) therapy and monitored for tumor response. Mice were sacrificed at day 6 or 12, and tumors were harvested for flow cytometry, as shown in Fig. 1A. Blood was collected via retroorbital bleed prior to irradiation, as well as on days 6 and 12 postirradiation. Plasma was isolated and IFNγ quantified using an ELISA kit (BioLegend® Inc., San Diego, CA) according to the manufacturer's instructions.

Immune Checkpoint Inhibitor Treatment (ICI)

Anti-PD1 and anti-CTLA4 antibodies were obtained from Bio X Cell® (Lebanon, NH). Three doses of antibodies were injected intraperitoneally on days 0, 2, and 6 postirradiation according to the scheme shown in Fig. 1. The doses administered were 200 μg anti-PD1 and 100 μg anti-CTLA4. For the groups where inoculation of abscopal tumors was delayed until the day of primary tumor irradiation, ICI was not studied.

Immunofluorescence Staining

Immunohistochemical staining was performed using an enclosed and humidified IHC chamber at the UAMS Cancer Institute (Little Rock, AK). Tumors were sectioned at 5-μm thickness. Tissue sections were blocked for 30 min with 2% bovine serum albumin and subsequently incubated with fluorescent-labeled antibodies (anti-CD8, anti-CD4, anti-CD11c, anti-PDL1) for 60 min.

Imaging and Analysis

Slides were viewed and imaged on an Olympus IX71 fluorescent microscope (Tokyo, Japan) at 40× resolution. Entire tissue sections were included in the analysis. Threshold was adjusted to exclude excessive background and stained regions were quantified by manual counting of individual cells.

Evaluation of Tumor-Infiltrating Immune Cells by Flow Cytometry

Tumors were excised on days 6 and 12 postirradiation and mechanically dissociated with shears until pieces were <1 mm^3. This was followed by enzymatic dissociation [1 mg ml^{-1} Collagenase, 2.5 U ml^{-1} Dispase (both from Invitrogen™, Carlsbad, CA) and 1 mg ml^{-1} DNaseI (Sigma-Aldrich® LLC, St. Louis, MO)] for 30 min with continuous agitation in a 37°C incubator. Subsequently the tissue suspensions were put on ice and cold FACS buffer (2% FBS in PBS) media was added. The samples were then sieved through a 70-μm cell strainer (BD Falcon™; BD Biosciences, Bedford, MA) fitted on a 50-ml tube on ice to

remove undigested cell clumps and separate the single cells. Cells were washed and collected by centrifugation at 300*g* for 5 min at 4°C (17). These were incubated in Fc block (BD Biosciences) for 20 min on ice in FACS buffer, then incubated with fluorophore-conjugated antibodies against CD4, CD8, CD25, CD44, CD69, PD-L1, CD80, CD86, CD11c, MHCII along with FVD 780 (for excluding dead cells) for 30 min on ice and washed three times with FACS buffer. Samples were then fixed in 2% formaldehyde for 15 min, washed and resuspended in FACS buffer and run on a flow cytometer at the UAMS flow core facility, and data were analyzed using FlowJo software (Ashland, OR) (fluorescence minus one (FMO) controls were used for setting up the gates).

RESULTS

Growth Response in Primary Tumors

After irradiation, tumor volumes were measured every 2–3 days until the final harvest on day 12 to assess changes in tumor growth. As shown in Fig. 3, tumors in untreated mice grew in volume 7.4-folds by day 12. Comparatively, tumors in mice receiving whole-tumor irradiation and immune checkpoint inhibitors (WTRT with ICI) averaged a 32% reduction in tumor volume by day 12 ($P = 0.0001$). The other groups achieved a significant degree of growth delay by day 12 as follows: WTRT alone and GRID alone had 3.32 and 3.04-fold increases in volume, respectively ($P = 0.001$, 0.0001); tumors on ICI alone grew 4.99-fold and the GRID with ICI tumors grew the least, 2.86-fold over control ($P < 0.002$, $P = 0.001$, respectively).

Effect of dual checkpoint blockade on primary tumor growth response.—Anti-PD1/anti-CTLA4 therapy alone showed an inferior response compared to radiation alone with either WTRT or GRID ($P = 0.03$, $P = 0.0002$ respectively). However, when combined with radiation (either GRID/ICI or WTRT/ICI) a more prominent reduction in primary tumor growth was observed. The most dramatic response was seen in WTRT/ICI where a persistent regression/stasis in tumor size was actually observed until the termination of the study ($P < 0.0001$).

Growth Response in Abscopal Tumors

Existing abscopal tumor on the day of irradiation.—As shown in Fig. 3, growth rates of abscopal, nonirradiated tumors in the majority of treatment groups were similar to those in control, untreated mice. However, in mice in which the primary tumor received 20 Gy GRID, evidence of an abscopal response was observed by day 12 of tumor measurement as illustrated by a reduction in average tumor volume (4.7-fold compared to 6.2-fold; $P < 0.001$). Compared to control mice, significant responses were not seen with ICI alone or with either combination of radiation (WTRT or GRID) and ICI.

Abscopal tumor inoculation on the day of irradiation.—When the abscopal tumor was implanted on the day of irradiation, substantial primary tumor growth inhibition was seen with whole tumor but not with spatially fractionated radiation (Fig. 2). The abscopal tumors in mice in which the primary tumor was treated with whole-tumor irradiation did not show any response, however those in mice with GRID-treated primary tumors showed

significantly decreased growth (Fig. 2) compared to the untreated group and compared to the WTRT group with an established abscopal tumor.

Profile of Infiltrated Immune Cells in Tumor

IHC analysis in both primary and abscopal tumors revealed that these abscopal growth changes were accompanied by a relative increase in CD8:CD4 ratio, suggesting a gross representation of cytotoxic T-cell expansion (Fig. 2C and D). A concomitant increase in $CD11c^+$ cells was also seen, suggesting a higher density of antigen-presenting cells such as dendritic cells in these tumors (data not shown). Abscopal tumors from both WTRT- and GRID-treated mice also showed a relative increase in PD-L1-expressing cells compared to controls (data not shown) as shown by IHC.

Immune infiltration with and without ICI treatment (existing abscopal tumors on day of irradiation).—Immune cell populations in abscopal tumors were analyzed using flow cytometry on days 6 and 12 postirradiation. Figure 4A and B shows proportions of activated $CD8^+$ and $CD4^+$ T cells across the experimental groups. Untreated mice showed an activated T-cell proportion of 44.2% ± 1.44 ($CD8^+CD44^+CD69^+$) and 25.6% ± 1.07 ($CD4^+CD44^+CD69^+$). In comparison, GRID-treated mice showed significantly increased levels of $CD8^+$ T-cell activation (73.2% ± 7.76, $P = 0.0002$) and $CD4^+$ T-cell activation (67.0% ± 10.7, $P = 0.02$) at day 12. Similarly, GRID with ICI-treated mice showed increases in $CD8^+$ T-cell activation (78.6% ± 3.1, $P = 0.02$) and $CD4^+$ T-cell activation (71.1% ± 5.99, $P = 0.001$). Such increases were appreciable at day 6 with $CD4^+$ T cells (GRID: 44.1% ± 2.5, $P = 0.001$; GRID with ICI: 48.5% ± 8.5, $P = 0.07$) but not with $CD8^+$ T cells. In comparison, WTRT and WTRT with ICI treatment groups did not show a significant increase in either subset of activated T cells. The relative change in both $CD8^+$ and $CD4^+$ T-cell activation from day 6 to day 12 across each treatment group can be seen in Fig. 4C. As shown here, it is apparent that there is a profound increase in these populations shown in GRID-treated mice (GRID alone or with ICI). Those treated with whole-beam radiation (WTRT alone or with ICI) or ICI alone showed the opposite trend, resulting in less relative T-cell activation at day 12 compared to GRID treatment groups.

MHCII was measured in a likewise fashion, with results shown in Fig. 5. The pattern observed appears complementary to that of T-cell activation, with relatively more MHCII positivity observed in GRID (60.6% ± 4.65 vs. 43.9% ± 0.77%, $P = 0.02$) or GRID with ICI (71.0% ± 1.95 vs. 43.9% ± 0.77%, $P < 0.001$) mice at day 12 compared to control mice and also in comparison to the other treatment groups including WTRT (42.9% ± 3.46, $P < 0.05$), WTRT with ICI [43.7% ± 1.09, $P < 0.05$) or ICI alone (52.1% ± 3.32, $P = 0.18$, $P = 0.001$ (GRID, GRID with ICI respectively)]. We also show that dendritic cells ($MHCII^+/CD11c^+$) were markedly increased in GRID-treated mice compared to untreated control (16.7% ± 2.67 vs. 0.2% ± 0.03, $P = 0.003$), ICI (0.2% ± 0.02, $P < 0.001$), WTRT (0.3% ± 0.10, $P < 0.001$), and WTRT with ICI (0.3% ± 0.10, $P = 0.003$) mice. GRID with ICI-treated mice also showed increases compared to control (15.9% ± 1.30 vs. 0.2% ± 0.03, $P < 0.001$), ICI (0.2% ± 0.02, $P < 0.001$), WTRT (0.3% ± 0.01, $P < 0.001$), and WTRT with ICI (0.3% ± 0.10, $P < 0.001$) mice.

Peripheral blood IFNγ concentration as a measure of systemic immune activation.—IFNγ concentration was measured in peripheral blood at day 0 (baseline, prior to intervention), followed by days 6 and 12 postirradiation. Figure 6 shows the relative concentration in each treatment group. Single-modality WTRT or ICI alone showed no significant change from baseline control values at both day 6 [261.4 ± 54.98 pg/ml vs. 256.2 ± 29.92 pg/ml, $P = 0.92$ (WTRT); 159.7 ± 29.59 pg/ml vs. 187.6 ± 39.22 pg/ml, $P = 0.06$ (ICI)] and day 12 [270.5 ± 93.51 pg/ml vs. 187.6 ± 39.22 pg/ml, $P = 0.44$ (WTRT); 240.5 ± 66.12 pg/ml vs. 256.2 ± 29.92 pg/ml, $P = 0.51$ (ICI)], suggesting no significant effect from these interventions. However, combination therapy with WTRT and ICI was associated with a nonsignificant rise in IFNγ at day 6 compared to baseline values (357.4 ± 77.3 pg/ml vs. 256.2 ± 29.92 pg/ml, $P = 0.30$). Notably, mice receiving GRID alone showed more substantial increases in IFNγ at day 6 compared to baseline (374.5 ± 92.3 pg/ml vs. 256.2 ± 29.92 pg/ml, $P = 0.15$), and the combination of GRID with ICI achieved the greatest increase in systemic IFNγ of all the intervention groups compared to baseline (463.7 ± 116.5 pg/ml vs. 256.2 ± 29.92 pg/ml, $P = 0.05$). By day 12, levels of IFNγ returned to their approximate baseline values in each of the groups.

PD-L1 Expression

PD-L1 expression was analyzed by flow cytometry on days 6 and 12 postirradiation in the nonirradiated abscopal tumor. Figure 7 shows the percentage of $PDL1^+$ cells in each radiation treatment group including measurements of control (untreated) mice at day 12 for comparison. While $PD\text{-}L1^+$ cells were present in each group at day 6, by day 12 $PD\text{-}L1^+$ measurements greater than 1% were observed only in GRID-treated mice (GRID or GRID with ICI). At day 12, $PD\text{-}L1^+$ cells in GRID-treated mice were significantly higher compared to untreated control (9.3% ± 3.6 vs. 0.4% ± 0.047, $P = 0.04$), WTRT (0.5% ± 0.21, $P = 0.05$), and WTRT with ICI (0.4% ± 0.12, $P = 0.09$) mice. PD-L1 in GRID with ICI-treated mice was also higher compared to untreated control (11.8% ± 5.65 vs. 0.4% ± 0.047, $P = 0.11$), WTRT (0.5% ± 0.21, $P = 0.12$), and WTRT with ICI (0.4% ± 0.12, $P = 0.18$) mice.

DISCUSSION

We combined the concept of spatial/partial tumor irradiation and immune checkpoint inhibitor treatment here to ascertain the potential of using GRID treatment as an immune adjuvant strategy in oncology and to compare with similar effects using whole-tumor irradiation. As expected from other studies reported in the literature, the combination of whole-beam radiation with anti-PD1/anti-CTLA4 therapy induced a substantial reduction in the size of primary tumor lesions, which persisted throughout the duration of the study. It is worth noting that the model used (4T1) is a fast-growing tumor, which did not allow us to completely assess long-term immunological effects beyond 2–3 weeks of tumor growth due to tumor progression in the untreated animals. Although the durability of the observed responses is not known, the degree of tumor regression suggests that continued application of these approaches might have long-term success in controlling the primary tumor.

Novel methods in radiation planning and delivery promote techniques such as stereotactic body radiation therapy (SBRT) as a curative option for patients with unresectable solitary tumors such as metastatic melanoma, pancreatic tumors or lung cancer. Recently published prospective data advocate its use in a broad clinical context including the management of metastatic lesions (1) or in combination with immune checkpoint blockade to optimize local responses (2). While these studies demonstrate efficacy in limiting disease progression, a clear method to also affect and potentially eradicate metastases has yet to emerge with SBRT. Our data in irradiated primary tumors suggest that combining spatially fractionated radiotherapy with dual immune checkpoint blockade may enhance clinical responses and also promote control via enhanced immune function against advanced disease in nonirradiated sites. While our study has not recapitulated complete treatment plans that would be engaged clinically, our data suggest that whole-tumor irradiation combined with immune checkpoint inhibition does less for the systemic control of disease than if GRID treatment is administered to the primary tumor in combination with immune checkpoint antibody treatment. A prominent question, for clinical studies that are now under design by a number of groups, is whether GRID to a primary tumor can help to maximally promote an anti-tumor immune response in humans in the context of subsequent standard fractionated chemoradiotherapy followed by surgical excision.

Our study of nonirradiated tumor responses demonstrates that GRID exposures can generate abscopal-like responses in beneficial immune cell infiltrate and tumor growth rate in the first week postirradiation. Perhaps most importantly, the intratumoral immune cell composition of abscopal tumors showed significantly increased amounts of both activated $CD4^+$ and $CD8^+$ T cells (Fig. 4). Our findings illustrate the beginnings of what appears to be a mounting anti-tumor immune effect that could be instrumental to developing long-term abscopal tumor control. Indications of a pro-tumor control immune cell phenotype began to emerge within days 12–14 postirradiation, and were able to be assessed before animals were required to be euthanized. Future studies in slower-growing, spontaneous tumor models would be extremely valuable in validating our initial observations here.

In addition, at day 6 postirradiation of the primary tumor, plasma concentrations of IFNγ in GRID-treated mice were significantly increased compared to other experimental groups utilizing combinations of whole-beam irradiation with or without checkpoint inhibitors. The increased immune cell activation and infiltration combined with this cytokine induction suggest that a systemic state of immune activation may be induced to a greater extent after GRID treatment compared to a whole-tumor large single dose. We also observed a significant increase in $MHCII^+$ positivity in abscopal tumors, including antigen-presenting cells (APCs) such as dendritic cells, macrophages and B cells. Interestingly, published clinical studies have suggested MHCII to be a predictive marker for response to immune checkpoint blockade in Hodgkin's lymphoma (33). In addition, we were able to show that conventional dendritic cells ($MHCII^+/CD11c^+$) were more abundant in abscopal tumors from GRID-treated mice compared to control or whole-beam irradiation. Though MHCII expression is not entirely exclusive to antigen presenting cells, together these findings could imply that immunogenic effects of GRID lead to increased antigen presentation, subsequent T-cell activation and general immune response against abscopal tumors. Alternatively, increased infiltration of APCs might represent subsequent events after massive tumor cell

death in the primary tumor rather than what would be viewed as a classical initiation of an immune response (34).

While more specific subsets were not defined in our analysis, other animal studies have shown that the generation of abscopal effects requires recruitment of BATF3-dependent dendritic cells to otherwise poorly immunogenic tumors, which are required for cross-priming of tumor-specific T lymphocytes (35). The trigger for this response appears to be the accumulation of intracellular dsDNA under the regulation of three-prime repair exonuclease 1 (TREX1) and was only observed after repeated doses (6 and 8 Gy) but not after a single 20 Gy dose, suggesting that a certain dose threshold may be required for successful DC recruitment and T-cell activation (21). The role of other immune cell populations such as fast-acting, innate natural killer (NK) cells and suppressive cells such as myeloid-derived suppressor cells (MDSC) or T-regulatory cells remain to be studied. Importantly, whether or not GRID increases the access of the immune system into the tumor microenvironment or simply does not induce as strong a suppressive immune response compared to whole-tumor irradiation remains to be determined.

Interestingly, Markovsky *et al.* reported recently that abscopal responses could occur when irradiating tumors with a limited, but significant, portion of tumor volume (50%) exposed to radiation (30). Though it is unknown whether the out-of-field responses in this study are mechanistically similar to our experiment, this lends additional support to further explore spatial fractionation as an immunologic tool in cancer therapy. It is important to note that the immunologic correlates in our study were preferentially elevated in only GRID-containing therapy, occurring in both GRID-treated mice as well as those receiving GRID with ICI. A somewhat unexpected result was observed with PD-L1 expression, an established biomarker for predicting response to anti-PD1 therapy, being higher than whole-tumor irradiation in abscopal tumors from both GRID and GRID with ICI-treated mice by day 12 in our study. In agreement with this rise is a published study that established that higher levels of IFNγ lead to increased expression of PD-L1 in tumors (36). We recognize that an abscopal, radiotherapy-driven upregulation of PD-L1 is not homologous to native microenvironmental regulation of PD-L1 and therefore may not have the same predictive value for treatment or progression (37). However, it is possible that treatment of primary tumors with GRID may upregulate PD-L1 at distant sites through the increase of IFNγ that we observed, which might actually render them more susceptible to anti-PD1 therapy and promote a more immune-permissive state (38, 39). Despite this, the mice that received GRID with ICI did not achieve as much regression in size of the abscopal tumors as anticipated, which may be partially due to the rapid growth of the nonirradiated tumor in this model, which overshadowed the effects that might be observed when the full spectrum of immune activation is allowed to develop (40). Likewise, clinical experience with ICI has shown that it is common to observe early “tumor flare,” described as pseudo-progression, which is considered an intratumoral inflammatory process that can last weeks to months before a favorable response is ultimately achieved (40, 41). The increase in the number of immune cells in the abscopal tumors makes it plausible that a similar phenomenon was at work in our study, and growth delay in abscopal tumors would have been more apparent using a model with more gradual tumor growth or extending the experiment beyond 12 days.

Our tumor model is also distinct from other models where a naturally occurring primary tumor spawns tumor-disseminated cells to distant organs that go through a phase of dormancy followed by a phase of growth. Irradiating the primary tumor may or may not lead to abscopal effects in these types of distant metastases. Our model is therefore more akin to treating one metastasis and inducing an abscopal effect in another oligomet or several other lesions.

SUMMARY

Our results suggest combining radiotherapy with dual immune checkpoint blockade may be synergistic and generate early, robust changes in the immune activation profile against primary and abscopal tumors. This effect occurs preferentially when primary tumors are treated with spatial fractionation compared to whole-tumor irradiation. While there was sustained regression in primary tumors utilizing conventional whole-beam irradiation with ICI, abscopal effects in terms of tumor growth rate and immune cell infiltrate were more pronounced after treatment of the primary tumor with spatially fractionated radiation. The latter may represent a new, clinically feasible tool for the improved control of metastatic disease. Capitalizing on this potential will require further study of dose responses and treatment sequencing and further elucidating the precise interactions occurring between cells not directly traversed by the radiation field and their subsequent impact on systemic immunologic activity. Other questions to be addressed include the impact of disease burden (location and volume of metastases) and how to possibly combine spatial fractionation with other immune-active agents, including cytokines, nanoparticles, or adoptive cell therapy. In view of the currently active NCI work/interest groups focused on the biology, physics and clinical aspects of spatial fractionation, there is strong motivation and rationale to include it in upcoming clinical studies.

ACKNOWLEDGMENTS

We thank the flow cytometry facility and the DLAM facility at the University of Arkansas for Medical Sciences for their accommodation to our studies. We thank the Department of Radiation Oncology, Division of Hematology and Oncology, and the Winthrop Rockefeller Cancer Institute for shared resources involved in conducting our studies. We also thank the Laura F. Hutchins, MD, Distinguished Chair for Hematology and Oncology for partial support of the study.

REFERENCES

1. Palma DA, Olson R, Harrow S, Gaede S, Louie AV, Haasbeek C, et al. Stereotactic ablative radiotherapy versus standard of care palliative treatment in patients with oligometastatic cancers (SABR-COMET): a randomised, phase 2, open-label trial. Lancet 2019; 393:2051–8. [PubMed: 30982687]
2. Theelen WSME, Peulen HMU, Lalezari F, van der Noort V, de Vries JF, Aerts JGJV, et al. Effect of pembrolizumab after stereotactic body radiotherapy vs pembrolizumab alone on tumor response in patients with advanced non-small cell lung cancer: Results of the PEMBRO-RT phase 2 randomized clinical trial. JAMA Oncol 2019; 5:1276–82.
3. Milano MT, Zhang H, Metcalfe SK, Muhs AG, Okunieff P. Oligometastatic breast cancer treated with curative-intent stereotactic body radiation therapy. Breast Cancer Res Treat 2009; 115:601–8. [PubMed: 18719992]
4. Formenti SC, Demaria S. Systemic effects of local radiotherapy. Lancet Oncol 2009; 10:718–26. [PubMed: 19573801]

5. Deng L, Liang H, Burnette B, Weicheslbaum RR, Fu YX. Radiation and anti-PD-L1 antibody combinatorial therapy induces T cell-mediated depletion of myeloid-derived suppressor cells and tumor regression. Oncoimmunology 2014; 3:e28499. [PubMed: 25050217]
6. Lugade AA, Sorensen EW, Gerber SA, Moran JP, Frelinger JG, Lord EM. Radiation-induced IFN-gamma production within the tumor microenvironment influences antitumor immunity. J Immunol 2008; 180:3132–9. [PubMed: 18292536]
7. Rodríguez-Ruiz ME, Vanpouille-Box C, Melero I, Formenti SC, Demaria S. Immunological mechanisms responsible for radiation-induced abscopal effect. Trends Immunol 2018; 39:644–55. [PubMed: 30001871]
8. Twyman-Saint VC, Rech AJ, Maity A, Rengan R, Pauken KE, Stelekati E, et al. Radiation and dual checkpoint blockade activate non-redundant immune mechanisms in cancer. Nature 2015; 520:373–7. [PubMed: 25754329]
9. Antonia SJ, Villegas A, Daniel D, Vicente D, Murakami S, Hui R, et al. Durvalumab after chemoradiotherapy in stage III non-small-cell lung cancer. N Engl J Med 2017; 377:1919–29. [PubMed: 28885881]
10. Ngwa W, Irabor OC, Schoenfeld JD, Hesser J, Demaria S, Formenti SC. Using immunotherapy to boost the abscopal effect. Nat Rev Cancer 2018; 18:313–22. [PubMed: 29449659]
11. Mole RH. Whole body irradiation; radiobiology or medicine? Br J Radiol 1953; 26:234–41. [PubMed: 13042090]
12. Terry NH, Travis EL. The influence of bone marrow depletion on intestinal radiation damage. Int J Radiat Oncol Biol Phys 1989; 17:569–73. [PubMed: 2528526]
13. Jia D, Gaddy D, Suva LJ, Corry PM. Rapid loss of bone mass and strength in mice after abdominal irradiation. Radiat Res 2011; 176:624–35. [PubMed: 21859327]
14. Jia D, Koonce NA, Griffin RJ, Jackson C, Corry PM. Prevention and mitigation of acute death of mice after abdominal irradiation by the antioxidant N-acetyl-cysteine (NAC). Radiat Res 2010; 173:579–89. [PubMed: 20426657]
15. Calveley VL, Khan MA, Yeung IW, Vandyk J, Hill RP. Partial volume rat lung irradiation: temporal fluctuations of in-field and out-of-field DNA damage and inflammatory cytokines following irradiation. Int J Radiat Biol 2005; 81:887–99. [PubMed: 16524844]
16. Poleszczuk JT, Luddy KA, Prokopiou S, Robertson-Tessi M, Moros EG, Fishman M, et al. Abscopal benefits of localized radiotherapy depend on activated T-cell trafficking and distribution between metastatic lesions. Cancer Res 2016; 76:1009–18. [PubMed: 26833128]
17. Jenkins SV, Robeson MS, Griffin RJ, Quick CM, Siegel ER, Cannon MJ, et al. Gastrointestinal tract dysbiosis enhances distal tumor progression through suppression of leukocyte trafficking. Cancer Res 2019; 79:5999–6009 [PubMed: 31591154]
18. Abuodeh Y, Venkat P, Kim S. Systematic review of case reports on the abscopal effect. Curr Probl Cancer 2016; 40:25–37. [PubMed: 26582738]
19. Formenti SC, Rudqvist NP, Golden E, Cooper B, Wennerberg E, Lhuillier C, et al. Radiotherapy induces responses of lung cancer to CTLA-4 blockade. Nat Med 2018; 24:1845–51. [PubMed: 30397353]
20. Grimaldi AM, Simeone E, Giannarelli D, Muto P, Falivene S, Borzillo V, et al. Abscopal effects of radiotherapy on advanced melanoma patients who progressed after ipilimumab immunotherapy. Oncoimmunology 2014; 3:e28780. [PubMed: 25083318]
21. Dewan MZ, Galloway AE, Kawashima N, Dewyngaert JK, Babb JS, Formenti SC, et al. Fractionated but not single-dose radiotherapy induces an immune-mediated abscopal effect when combined with anti-CTLA-4 antibody. Clin Cancer Res 2009; 15:5379–88. [PubMed: 19706802]
22. Kawakubo M, Demehri S, Manstein D. Fractional laser exposure induces neutrophil infiltration (N1 phenotype) into the tumor and stimulates systemic anti-tumor immune response. PLoS One 2017; 12:e0184852. [PubMed: 28922374]
23. Yovino S, Kleinberg L, Grossman SA, Narayanan M, Ford E. The etiology of treatment-related lymphopenia in patients with malignant gliomas: modeling radiation dose to circulating lymphocytes explains clinical observations and suggests methods of modifying the impact of radiation on immune cells. Cancer Invest 2013; 31:140–4. [PubMed: 23362951]

24. Laissue JA, Blattmann H, Slatkin DN. Alban Kohler (1874–1947): Inventor of grid therapy. Z Med Phys 2012; 22:90–9. (Article in German) [PubMed: 21862299]
25. Billena C, Khan AJ. A Current review of spatial fractionation: Back to the future? Int J Radiat Oncol Biol Phys 2019; 104:177–87. [PubMed: 30684666]
26. Liberson F. The value of a multi-perforated screen in deep X-ray therapy. Radiology1933; 20.
27. Yan W, Khan MK, Wu X, Simone CB, Fan J, Gressen E, et al. Spatially fractionated radiation therapy: History, present and the future. Clin Transl Radiat Oncol 2020; 20:30–8. [PubMed: 31768424]
28. Griffin RJ, Ahmed MM, Amendola B, Belyakov O, Bentzen SM, Butterworth KT, et al. Understanding high-dose, ultra-high dose-rate and spatially fractionated radiotherapy. Int J Radiat Oncol Biol Phys 2020; Epub ahead of print.
29. Asur R, Butterworth KT, Penagaricano JA, Prise KM, Griffin RJ. High dose bystander effects in spatially fractionated radiation therapy. Cancer Lett 2015; 356:52–7. [PubMed: 24246848]
30. Markovsky E, Budhu S, Samstein RM, Li H, Russell J, Zhang Z, et al. An antitumor immune response is evoked by partial-volume single-dose radiation in 2 murine models. Int J Radiat Oncol Biol Phys 2019; 103:697–708. [PubMed: 30342090]
31. Sharma S, Moros EG, Boerma M, Sridharan V, Han EY, Clarkson R, et al. A novel technique for image-guided local heart irradiation in the rat. Technol Cancer Res Treat 2014; 13:593–603. [PubMed: 24000983]
32. Zhang X, Penagaricano J, Yan Y, Liang X, Morrill S, Griffin RJ, et al. Spatially fractionated radiotherapy (GRID) using helical tomotherapy. J Appl Clin Med Phys 2016; 17:396–407. [PubMed: 26894367]
33. Roemer MGM, Redd RA, Cader FZ, Pak CJ, Abdelrahman S, Ouyang J, et al. Major histocompatibility complex class II and programmed death ligand 1 expression predict outcome after programmed death 1 blockade in classic hodgkin lymphoma. J Clin Oncol 2018; 36:942–50. [PubMed: 29394125]
34. Palucka K, Banchereau J. Cancer immunotherapy via dendritic cells. Nat Rev Cancer 2012; 12:265–77. [PubMed: 22437871]
35. Vanpouille-Box C, Alard A, Aryankalayil MJ, Sarfraz Y, Diamond JM, Schneider RJ, et al. DNA exonuclease Trex1 regulates radiotherapy-induced tumour immunogenicity. Nat Commun 2017; 8:15618. [PubMed: 28598415]
36. Chen S, Crabill GA, Pritchard TS, McMiller TL, Wei P, Pardoll DM, et al. Mechanisms regulating PD-L1 expression on tumor and immune cells. J Immunother Cancer 2019; 7:305. [PubMed: 31730010]
37. Shen X, Zhang L, Li J, Li Y, Wang Y, Xu ZX. Recent findings in the regulation of programmed death ligand 1 expression. Front Immunol 2019; 10:1337. [PubMed: 31258527]
38. Topalian SL, Hodi FS, Brahmer JR, Gettinger SN, Smith DC, McDermott DF, et al. Safety, activity, and immune correlates of anti-PD-1 antibody in cancer. N Engl J Med 2012; 366:2443–54. [PubMed: 22658127]
39. PD-L1 blockade maintains irradiation-mediated antitumor immunity. Cancer Discov 2014; 4:OF16.
40. Fuentes-Antras J, Provencio M, Diaz-Rubio E. Hyperprogression as a distinct outcome after immunotherapy. Cancer Treat Rev 2018; 70:16–21. [PubMed: 30053725]
41. Bourhis J, Sozzi WJ, Jorge PG, Gaide O, Bailat C, Duclos F, et al. Treatment of a first patient with FLASH-radiotherapy. Radiother Oncol 2019; 139:18–22. [PubMed: 31303340]

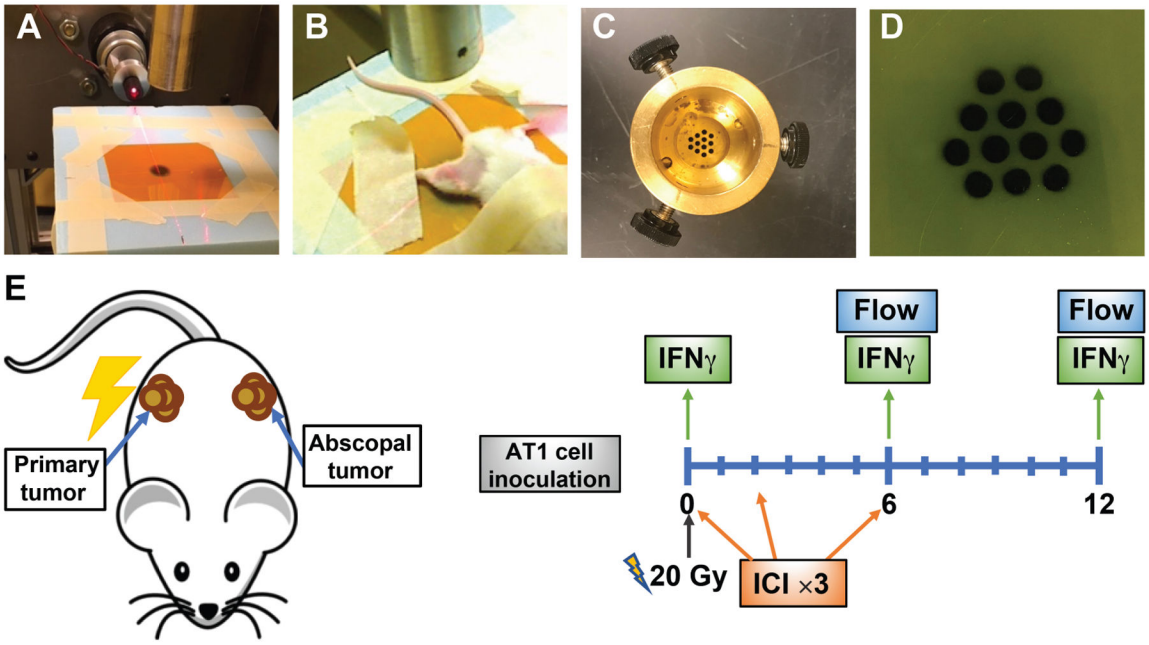

FIG. 1.

Irradiation setup. Panel A: Preirradiated film in position for whole-tumor irradiation. Panel B: Mouse in the treatment position. Panel C: GRID collimator. Panel D: GRID irradiated film. Panel E: Schematic representation of the experiment design. Shown here are mice with primary and abscopal tumors implanted on the same day. Additional analysis of mice with abscopal tumors implanted on the day of irradiation are not shown here.

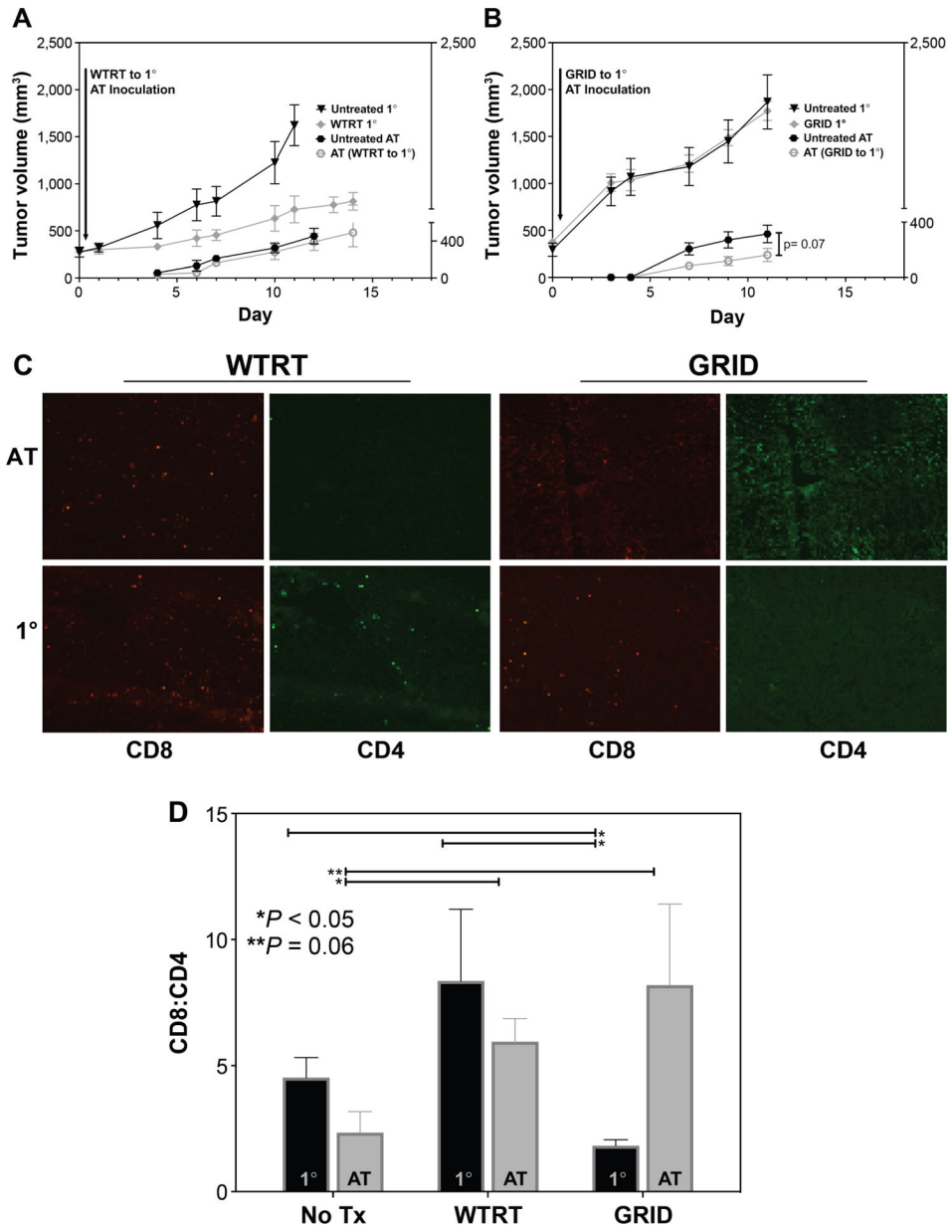

FIG. 2.

Tumor growth curves when abscopal (nonirradiated) tumors were inoculated on the day of primary (1°) tumor irradiation. Each group consisted of 5–8 4T1-bearing mice and the error bars represent ±1 SEM. Panel A: Comparable growth rates in abscopal tumors after whole-beam irradiation to the primary (1°) tumors. Panel B: Decreased growth rate of abscopal tumors after GRID to the primary (1°) tumors. Panel C: Immune cell composition with selected IHC images in primary (1°) and abscopal tumors from WTRT-treated mice and GRID-treated mice. Panel D: Post-treatment changes in CD8:CD4 ratio in primary (1°) vs. abscopal tumors.

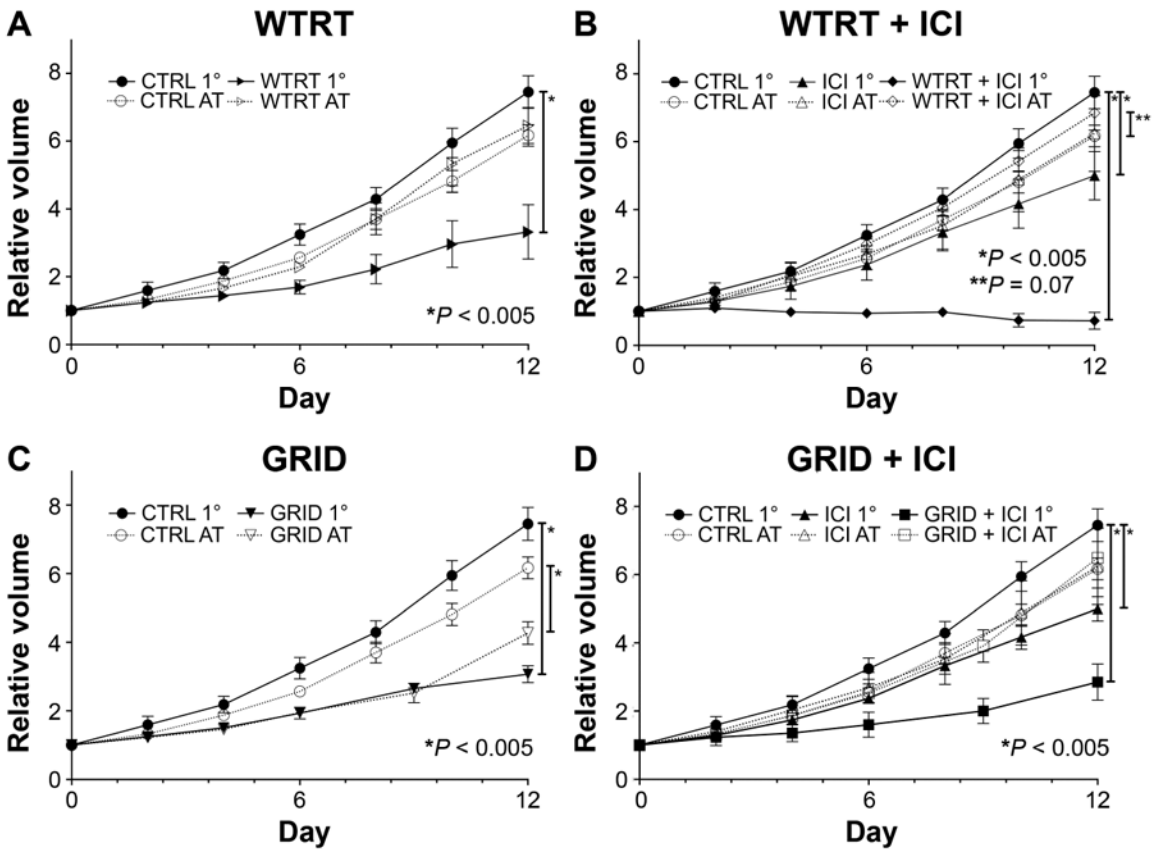

FIG. 3.

Comparison of tumor growth for (panels A–D) WTRT, WTRT + ICI, GRID and GRID + ICI, respectively, in primary (1°) (irradiated) or abscopal (nonirradiated) lesions. Each group consisted of 5–8 4T1-bearing mice and error bars represent ±1 SEM.

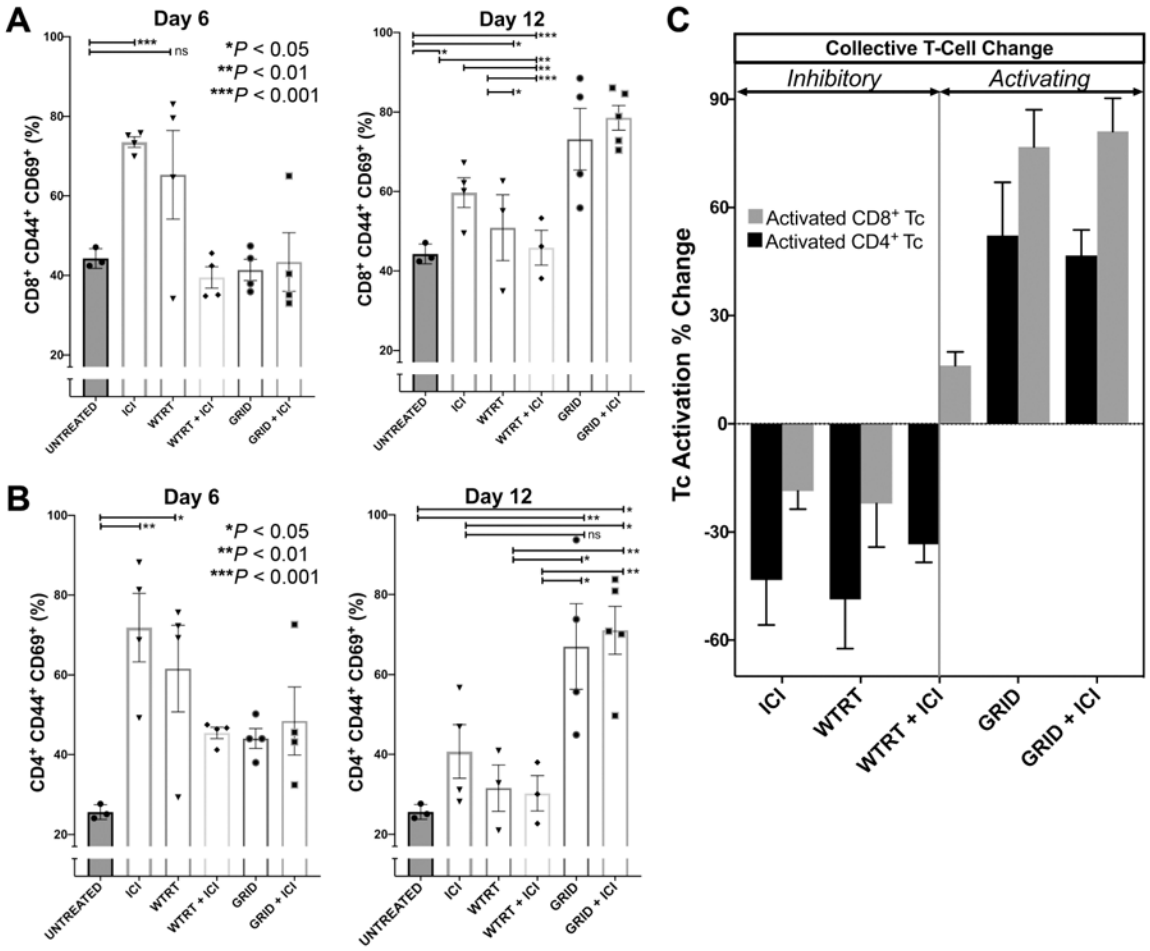

FIG. 4.

Panels A and B: $CD8^+$ and $CD4^+$ T-cell activation, respectively, in a nonirradiated tumor at day 6 and day 12. Each group consisted of 5–8 4T1-bearing mice and error bars represent ± 1 SEM. Panel C: Collective T-cell activation changes in nonirradiated tumor from day 6 to day 12.

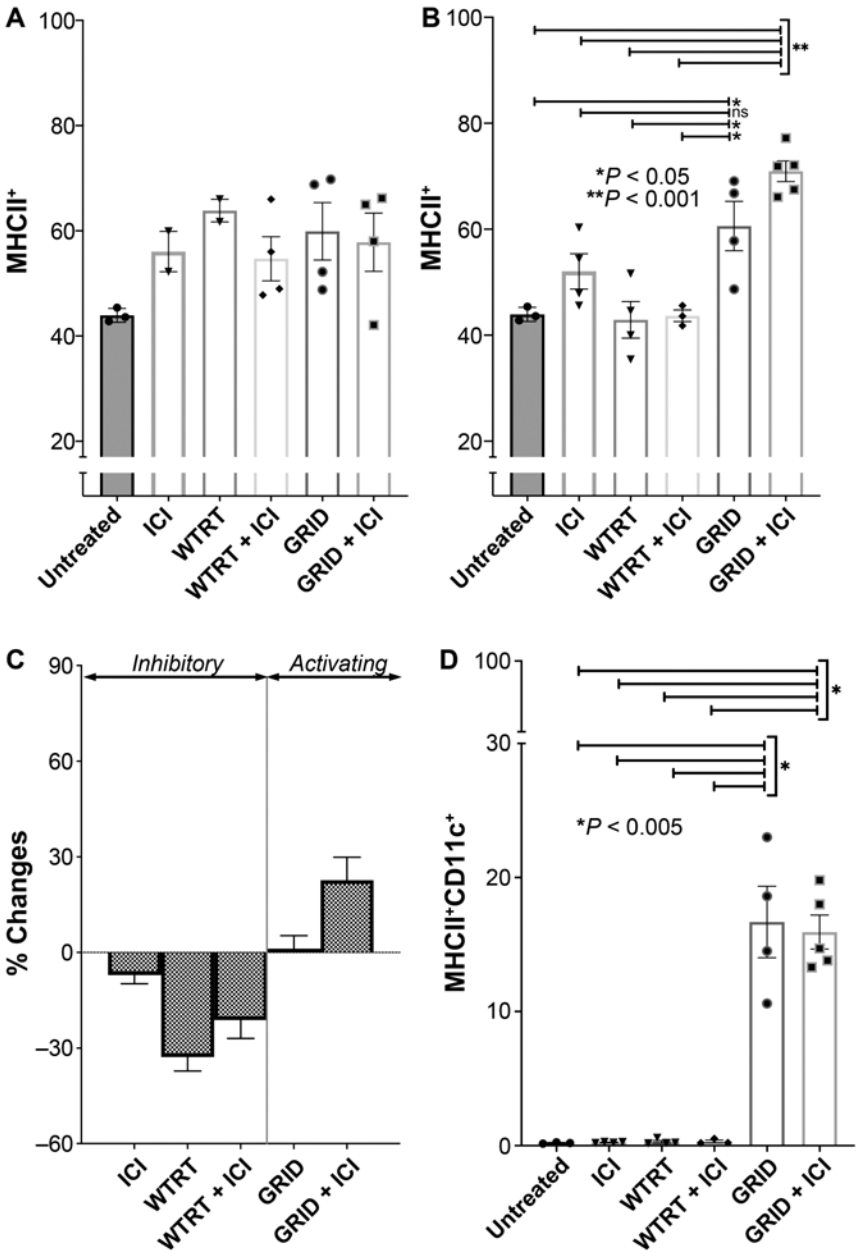

FIG. 5.

Panels A and B: MHCII$^+$ cells in abscopal tumors measured at day 6 and day 12, respectively. Each group consisted of 5–8 4T1-bearing mice and error bars represent ±1 SEM. Panel C: Collective MHCII$^+$ changes from day 6 to day 12. Panel D: Dendritic cells (MHCII$^+$/CD11c$^+$) in abscopal tumors at day 12.

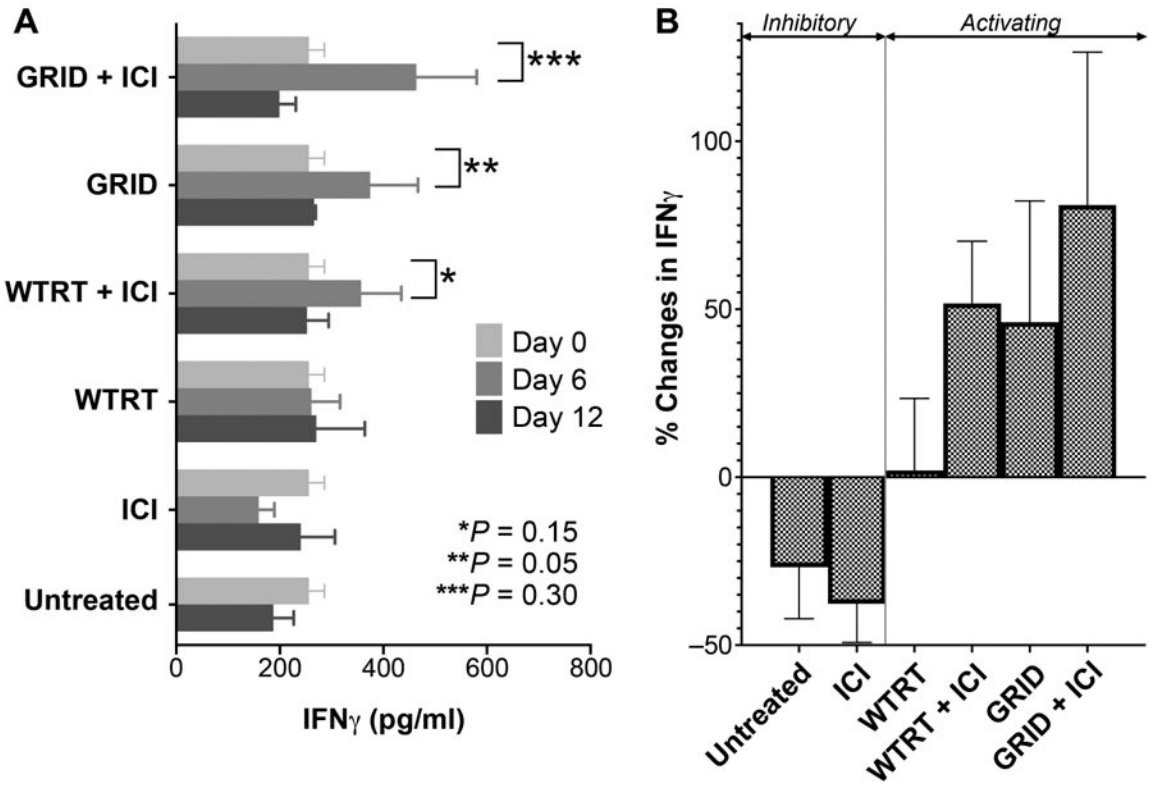

FIG. 6.

Panel A: IFNγ concentration in blood. Each group consisted of serum samples from 5–8 4T1-bearing mice and error bars represent ±1 SEM. Panel B: Collective change in IFNγ concentration from each treatment group at day 6 compared to baseline. Note that untreated mice were measured only at baseline and at day 12

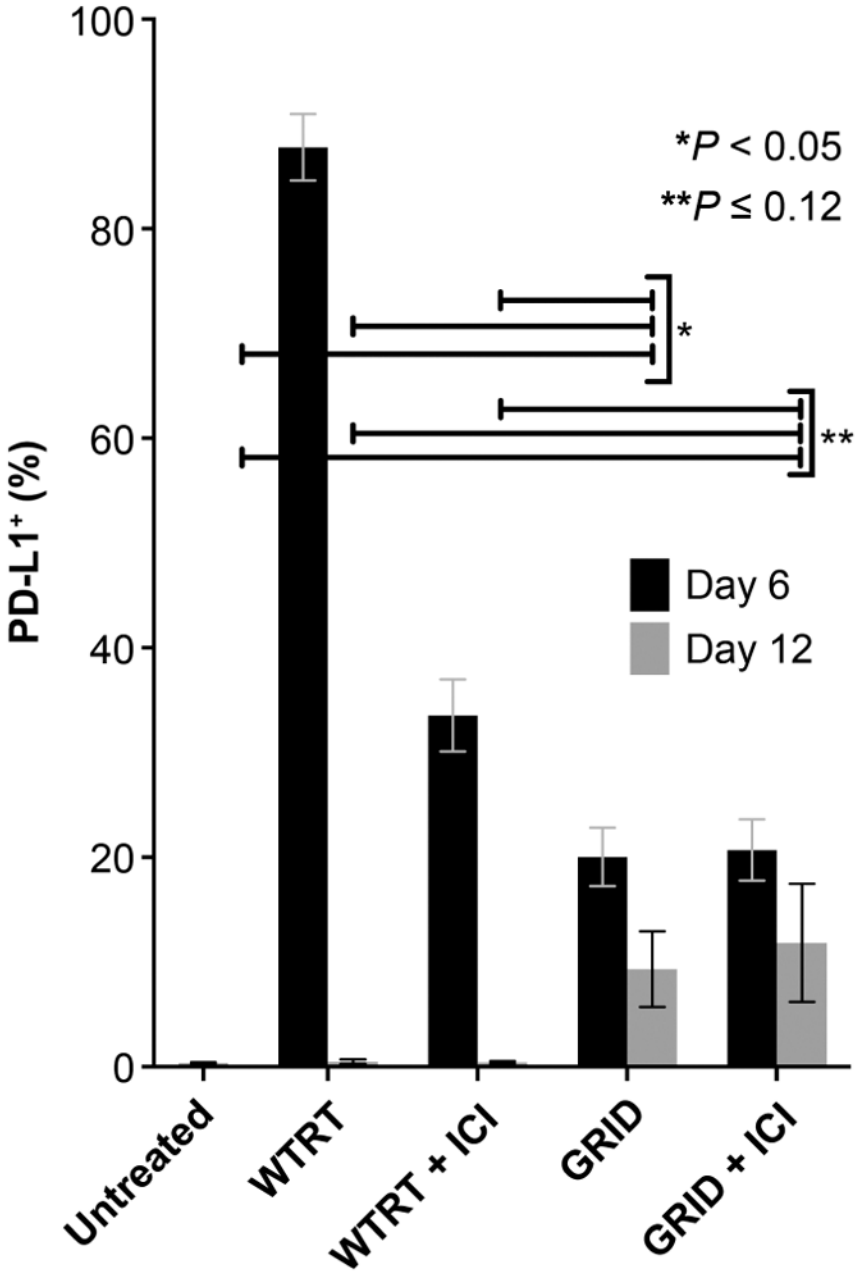

FIG. 7.

PD-L1% measured by flow cytometry in the nonirradiated tumor cell population at day 6 and day 12. Each group consisted of 5–8 4T1-bearing mice and error bars represent ±1 SEM.